Yong Zhao
Engineering Mechanics Group
Battelle Memorial Institute
505 King Avenue
Columbus, OH 43201

John D. Stevenson
Stevenson and Associates
9217 Midwest Avenue
Cleveland, OH 44125

H. T. Tang
Electric Power Research Institute
Department of Nuclear Safety
PO Box 10412
Palo Alto, CA 94303

Parametric Nonlinear Finite Element Analysis of Strain Ratcheting in Pressurized Elbows Based on Random Vibration

The large strain ratcheting in cyclic plasticity of a typical pressurized pipe elbow in a realistic nuclear piping system was investigated in a more quantitative manner than previously. The elbow was modeled using a fine mesh of shell elements that can provide the completed information of detailed time varying strain distributions in the whole elbow area. The nonlinear time history stress analyses performed were based on a pseudostatic concept using the vector-valued stochastic displacement response time series loaded at the elbow ends. The response time series were synthesized using a simulation approach based on the random vibration analyses of the piping system and its supporting building. After a finite element mesh convergence study, parametric analyses were conducted that included the effects due to the magnitude changes in excitation level, internal pressure, material yield stress, and material strain hardening. © *1996 John Wiley & Sons, Inc.*

INTRODUCTION

Strain ratcheting behavior and effects in cyclic plasticity are ongoing safety margin topics with respect to the excessive conservatism issues of current seismic design of nuclear piping under strong earthquake loads. The American Society of Mechanical Engineers Boiler & Pressure Vessel Code Section III (ASME BPVC, 1992) is undergoing changes in its nuclear piping design rules and stress criteria (Tagart and Ranganath, 1992; Slagis, 1993; Barnes, et al., 1994), because recent experimental and analytical research (General Electric, 1990; Park, 1991; Severud, 1988; Kot, 1990; Scavuzzo, 1993; Garud, 1993; Boussaa, et al., 1993a,b; Azzam and Scavuzzo, 1991; Azzam, 1992; Kussmaul, 1987; Beaney, 1991; Jaquay et al., 1991) demonstrated that the failure mechanism of a ductile steel piping under high level dynamic loads is governed by a ratcheting and fatigue mode rather than by the plastic collapse mode that was originally considered the principle basis of the Code rules and criteria. Such ratcheting and fatigue failure often occurs in the local strain concentration areas of piping elbows. The ratcheting behavior is due to material ductility and hardening and elbow geometrical ovalization of deformation under a cyclic

Received January 10, 1996; Accepted for publication March 27, 1996.

Shock and Vibration, Vol. 3, No. 5, pp. 373–387 (1996)

CCC 1070-9622/96/050373-15

loading. The ratcheting plastic strain may accumulate up to 1.0–5.0% or higher for about 10 cycles of high level loading without leading to a significant ratcheting-fatigue failure of the piping. Such high strain values are at least eight times the stress limit of the current Code Level D service condition and are excessively conservative relative to the supporting building that has generally a typical seismic safety margin of four. The local plastic ratcheted deformation causes load redistribution but does not significantly affect the global stiffness of the overall piping system that remains elastic. The ratcheting is self-limiting due to material hardening that absorbs most of the kinetic energy input to the dynamic piping system.

Due to the effects of high material nonlinearity and strain hardening in an elbow under strong cyclic loadings, it is not practical to perform a theoretical study. Rather, a nonlinear finite element analysis constitutes a feasible alternative approach. For a detailed analysis of localized ratcheting behavior a more accurate shell element type model is needed to provide the completed information of time varying principal strain distributions or strain contours in the whole area of the elbow. This information is necessary for further insight into the ratcheting behavior and for a more rational evaluation of the overly excessive seismic safety margin issues of nuclear piping design. However, this information is not available in physical tests of elbows in the literature. The approach using a shell element mesh is, in general, complicated and expensive in computation such that most researchers performed approximate numerical analyses using somewhat simplified pipe or elbow type elements to model the elbow. Such simplified analyses may not effectively evaluate the realistic local ratcheting behavior of the elbow with sufficient accuracy. No numerical results of large cyclic strain ratcheting in an elbow using a sophisticated shell element mesh are available in the literature.

On the other hand, the strain ratcheting of an elbow in a pressurized piping system is caused by earthquake type dynamic loads that are known to be quite random in nature. However, few ratcheting studies and results available in the literature are based on more rational but somewhat difficult random vibration approaches and results. The loads input in the ratcheting analyses by most researchers are one of the following: floor response spectra or time histories generated by assuming all the state variables and response components to be statistically independent; assumed in-plane or out of plane symmetrical bending moments; and direct use of free field ground excitations. It remains an issue to use these loads to more accurately evaluate the safety margins of a realistic nuclear piping housed by a building and anchored on different elevations or floors of a building, because the responses of the building and piping are actually nonstationary, vector-valued, and cross-correlated stochastic processes. Neglecting such correlation effects generally leads to a conservative prediction of the piping responses as found by Zhao (1993). The physical piping test results of ratcheting also need to be explained using a more sophisticated numerical approach.

The overall objective of the study presented in this article was to investigate the complicated large cyclic strain ratcheting phenomena in a typical pressurized elbow using a fine mesh of shell elements and a pseudostatic concept. The pressurized elbow was loaded at its ends using the prescribed multiaxial displacement response time series that are vector-valued, nonstationary, and cross-correlated stochastic processes (obtained by Zhao, 1993) directly at the elbow ends through the random vibration analyses of a realistic full-scale building and piping system and the autoregressive AR(p) simulation (Box and Jenkins, 1976; Shiao, 1986). Various cases were examined using varying parameters of excitation level, internal pressure, yield stress, and strain hardening.

MODELING AND ANALYSES

As mentioned in the previous section, the detailed finite element analysis of the large cyclic strain ratcheting behavior of an elbow using a shell element type mesh is very complicated in convergence and expensive in computation. This is true in particular when using a PC. To this end the number of shell elements used should be as few as possible if there is no mesh convergence problem for this model.

A mesh convergence calibration is especially necessary for developing a complicated nonlinear finite element model before a formal numerical calculation for a reliable and convergent result. Figures 1 and 2 show two nonlinear shell element models of a 2-in. Schedule 40 long radius elbow that were developed for this study. One model consists of a total of 432 [=three sectors (0°–37.5°, 37.5°–52.5°, and 52.5°–90°) × 4 circulus per sector

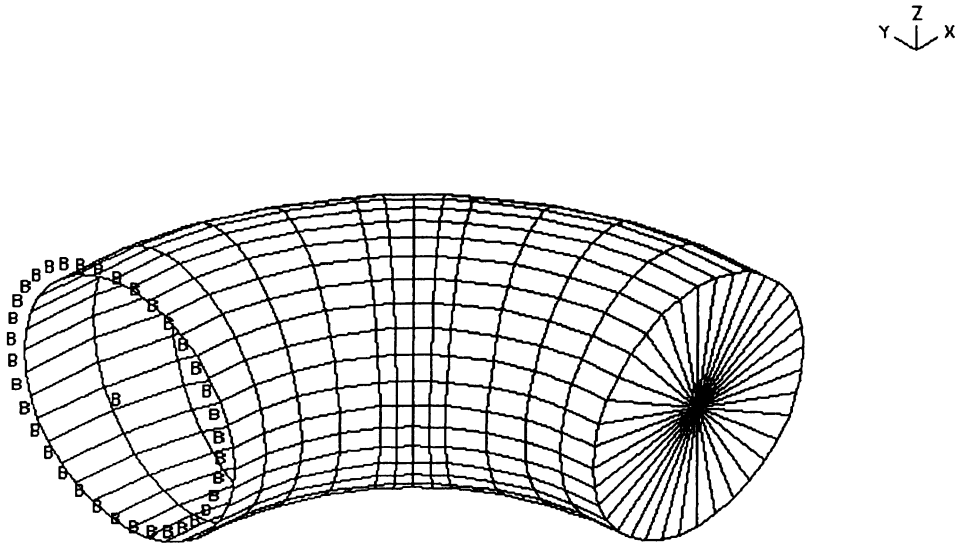

FIGURE 1 Finite element model of a 2-in. Sch. 40 standard elbow with 432 shell elements.

in the axial direction × 36 elements per circulus in the hoop direction] 4-node shell elements for the elbow shell and 16 triangular plate elements for the elbow cover plate put at one elbow end for loading purpose, and the other one of 648 (=3 × 36 × 6) 4-node shell elements and 16 triangular plate elements. For both the models, there is a finer element mesh at the center 15° region, and the elbow is fixed at one end and loaded at the center of the other free end cover plate with an in-plane cyclic bending time history that has a 1.4-s duration of one- and three-quarter cycles and a peak value of 2000 lb-in. (Fig. 3). The thickness of the cover plate was chosen such that it did not affect the strains calculated in the center area of the elbow and there was no ovalization at the end edge. The elbow was pressurized internally with a pressure of 1,350 psi that caused a hoop stress of 0.18 times the allowable design stress intensity value, S_h, for class 2 piping (ASME BPVC, 1992).

The general purpose nonlinear finite element code SOLVIA (1990) was employed to perform the pseudostatic time history analyses. SOLVIA

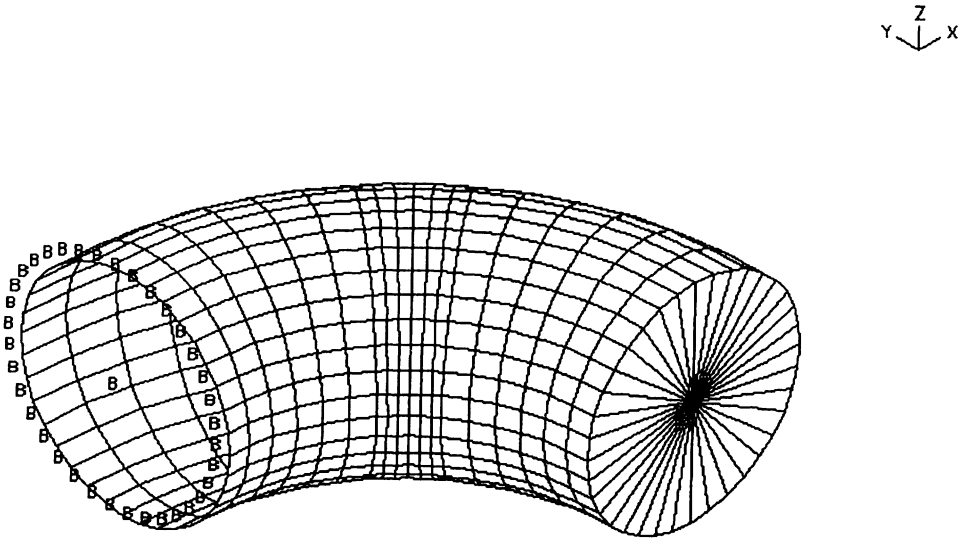

FIGURE 2 Finite element model of a 2-in. Sch. 40 standard elbow with 648 shell elements.

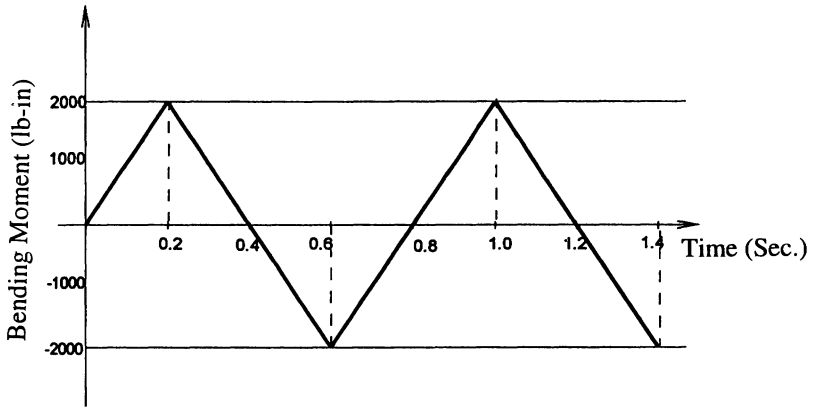

FIGURE 3 Typical in-plane bending forcing time history.

has been commercial for over 5 years and was developed on the basis of the ADINA program that has been used for nonlinear problems for more than 15 years. A 2 × 2 Gauss numerical integration order in surface and a Gauss integration order of 2 in thickness were adopted for the four-node shell elements. The equilibrium iteration method used in the numerical solution was the Broyden–Fletcher–Goldfarb–Shanno (BFGS) matrix update method with line searches. A tolerance type of energy and displacement convergence criterion was defined. A time step of 0.005 s and an autostep scheme were specified based on the iteration history. For the shell element type, the SOLVIA code provided a Mises yield surface with an isotropic hardening option only rather than kinematic hardening. However, the numerical comparisons using the ABAQUS code (Jaquay et al., 1991) indicated that the isotropic hardening rule could be used to predict elbow ratcheting with sufficient accuracy. A bilinearized stress–strain constitutive law of carbon steel SA-106B at 200F was assumed on the basis of tests by Rockwell International (1990) as shown in Fig. 4. A yield stress of 60.1 ksi, an elastic modulus of 2.9 × 10^7 psi, and a strain hardening or tangent modulus of 3.2 × 10^6 psi were specified.

The numerical stress and strain results obtained at various nodal points of the two models were examined. The critical part was found at the symmetrical section 45° away from the elbow end (Fig. 5). Typical comparisons of hoop and axial strains obtained for the two models on the symmetrical section defined in Fig. 5 indicate that the strains at the typical points are almost identical and convergent with relative differences of less than 1% between these two models, one of which has 50% more shell elements than the other. Similar conclusions can be obtained at other points of the elbow. Therefore, the element mesh defined in the 432 shell element model is sufficiently fine

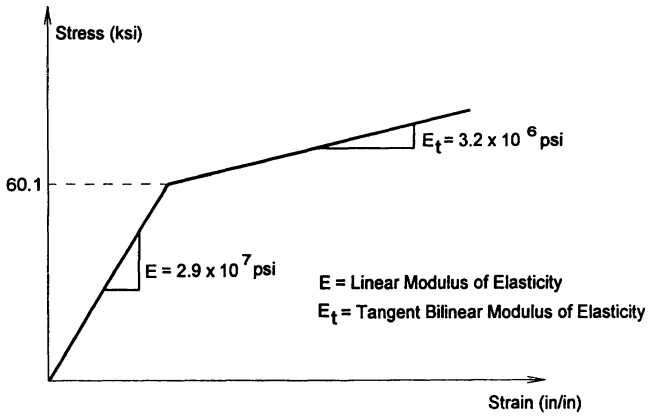

FIGURE 4 Stress–strain relation of SA-106B carbon steel at 200F.

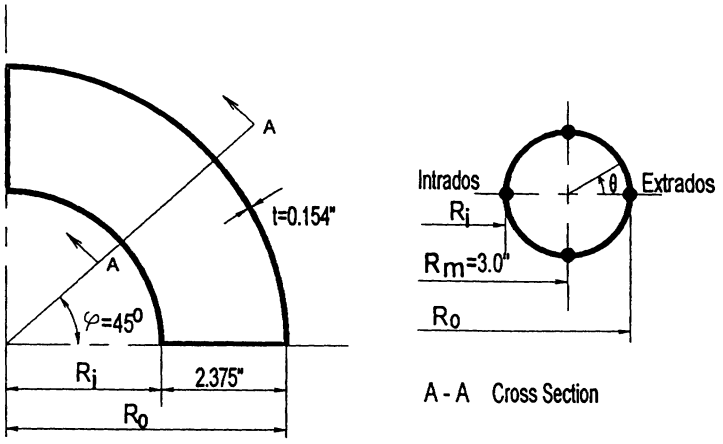

FIGURE 5 Four typical point locations on the 45° cross section of a 2-in. Sch. 40 standard elbow.

without a mesh convergence problem. This convergent mesh of the shell element can be used further for detailed nonlinear finite element analyses of large strain ratcheting in an elbow with more complicated loading and material cases.

A 2-in. Sch. 40 long radius elbow was found to be one of the most critical components of a realistic nuclear piping system mounted inside a four-story nuclear building by use of the random vibration modal time history (RVMTH) analyses (Zhao, 1993). Twelve-dimensional nonstationary and correlated piping displacement response time series (Fig. 6) that include the effects of inertia (primary term) and relative support motion (secondary term) were obtained by Zhao (1993) at the two ends of the elbow, using the time lag cross-covariance matrices of the piping displacement responses from the RVMTH analyses and extend-

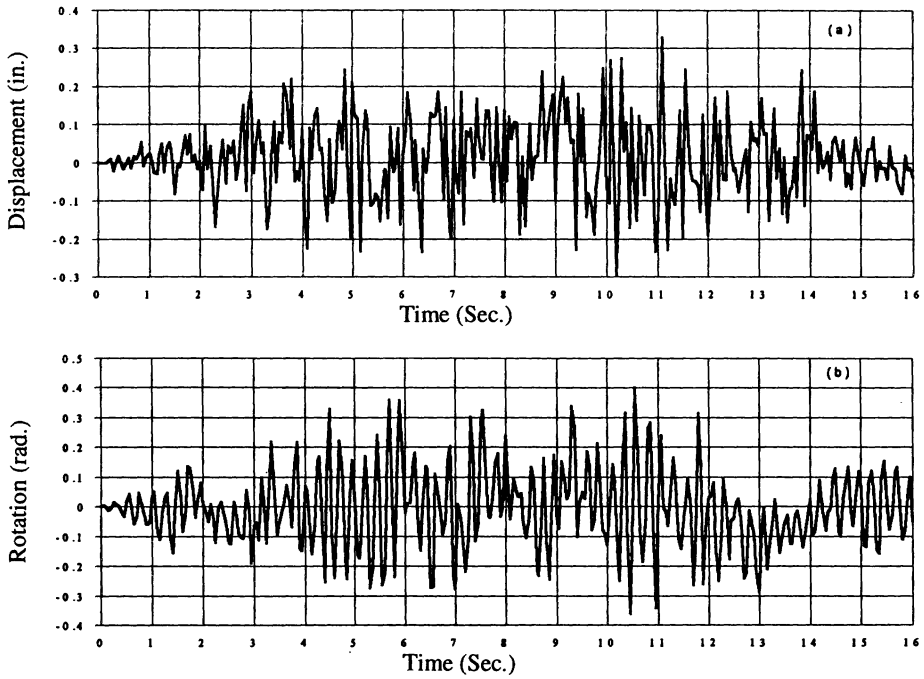

FIGURE 6 Typical prescribed multiaxial stochastic displacement time series at one elbow end with (a) translation in the x direction and (b) rotation in the xx direction.

ing the auto regressive AR(p) simulation formulation by Box and Jenkins (1976) and Shiao (1986). The synthesized stochastic time series of the displacement responses are unsymmetrical, primarily due to the effects of the unsymmetrical piping layout.

The nonlinear finite element model of the 2-in. Sch. 40 standard elbow with a 432 shell element mesh (shown in Fig. 1) was employed to perform pseudostatic nonlinear time history analyses using the SOLVIA code (1990). For computing simplicity purposes, the elbow was fixed at one end and loaded at the center of the other free end cover plate (Fig. 7) with 6-dimensional prescribed displacement time series with a 16-s duration. The displacement time series applied were computed from the differences of the associated displacements (Fig. 6) that are realistic piping responses at the two elbow ends. This simplified model is equivalent to the elbow loaded directly at the two ends with the associated displacement time series. The elbow was pressurized internally with a pressure of 1350 psi that caused a hoop stress of $0.18S_h$. A time step of 0.008 s and an autostep scheme were specified based on the iteration history. The same Gauss numerical integration order, the BFGS equilibrium iteration method, the convergence criteria, and the isotropic hardening option were adopted herein as those used in the mesh convergence study mentioned above. The same carbon steel SA-106B at 200F was assumed to have the same material properties as those listed previously and shown in Fig. 4.

Several parametric finite element analyses with different loading and material properties of the elbow model were conducted for a sufficiently detailed investigation of ratcheting behavior in cyclic plasticity. The analyses included a basic case of using the actual cyclic displacement loading plus the internal pressure loading and material properties listed above and nine comparison cases with parameter changes relative to the basic case as follows:

1. the cyclic loads were scaled down five times;
2. the cyclic loads were scaled down 10 times;
3. the cyclic loads were scaled up two times;
4. the cyclic loads were scaled up three times;
5. the cyclic loads were scaled up four times;
6. the pressure hoop stress was equal to zero;
7. the pressure hoop stress was equal to $1.0S_h$;
8. the steel yield stress was reduced to 35 ksi; and
9. the tangent modulus of elasticity of the steel was reduced two times.

The numerical results associated with the basic case and nine parametric study cases are presented in the next section.

RESULTS AND DISCUSSION

For the basic case with the actual displacement loading and material properties, the internal pressure of 1350 psi caused a hoop stress equal to $0.18S_h$. The S_h was equal to 0.429 times the yield stress that was 60.1 ksi in this case. Strain contours at any desired time were obtained by means of using the shell element model. The strain contours gave completed information of time varying

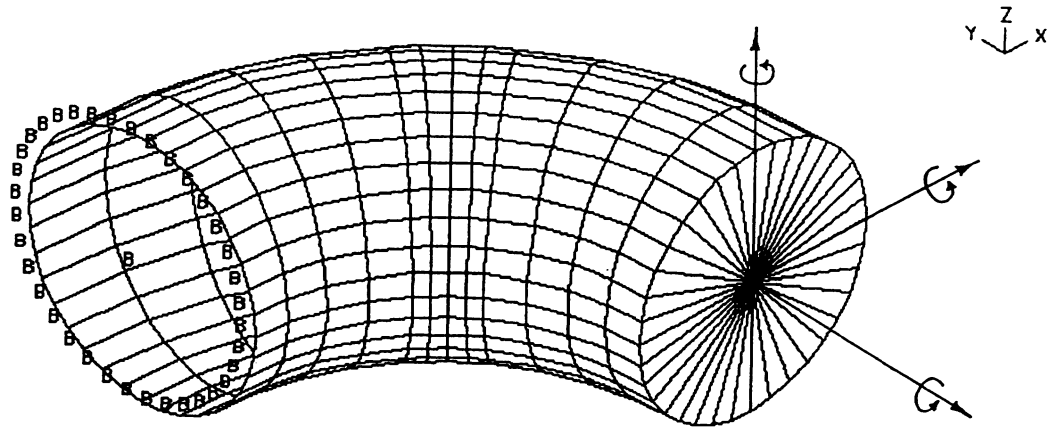

FIGURE 7 432 shell element finite element model of a 2-in. Sch. 40 standard elbow subject to 6-dimensional prescribed displacement time series.

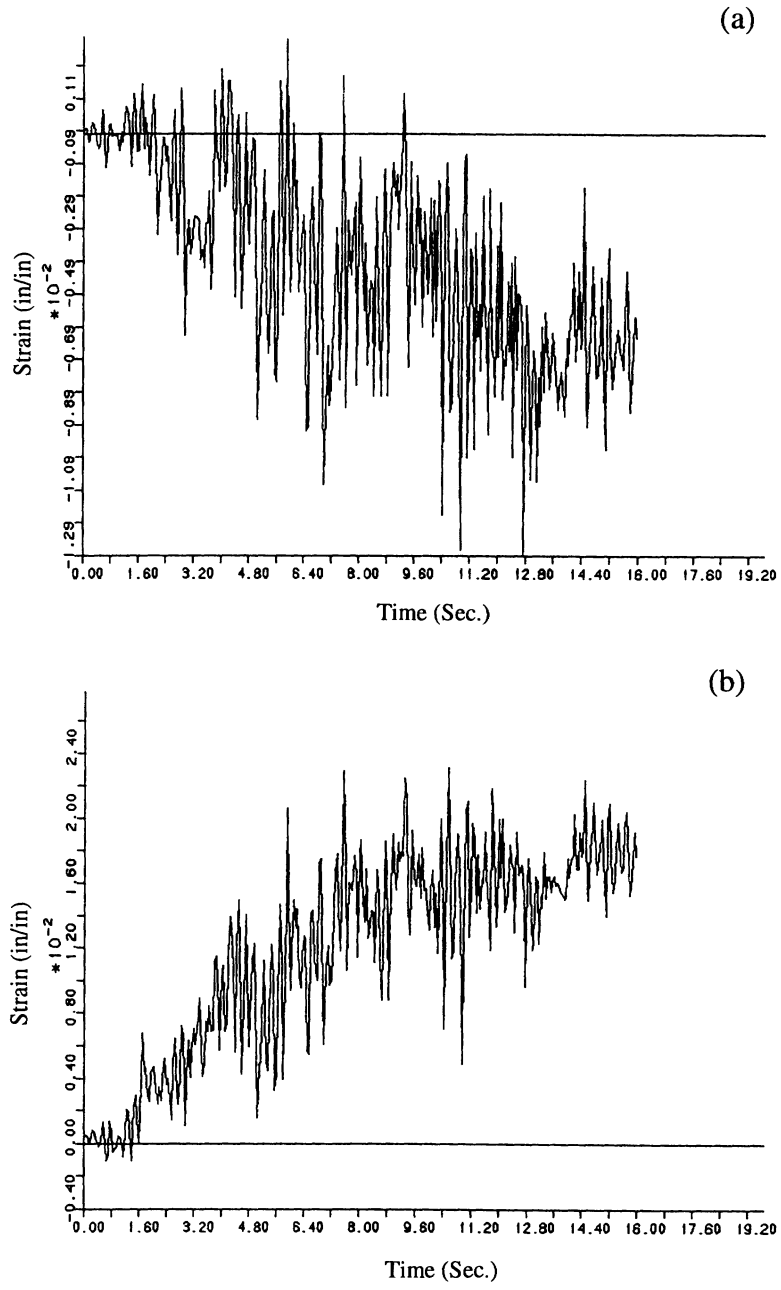

FIGURE 8 (a) Axial strain at the 0° point and (b) hoop strain at the 180° Point on the cross section 45° away from the elbow end under actual cyclic loads.

principal strain distributions in the whole elbow area. This information was necessary for a better understanding of the ratcheting behavior of the elbow, but was not available in physical tests and either using simplified pipe or elbow elements to model the elbow. The strain contours indicated that larger strains existed at the intrados location (180°) on the symmetrical section (Fig. 5) than other areas. Hence, attention should be paid to the central region where a finer shell element mesh was specially defined for this purpose as shown in Fig. 7.

Figure 8 presents typical axial and hoop stresses and strains at the four typical points on the symmetrical section 45° away from the elbow end (Fig. 5). On the symmetrical section, no stress ratcheting was found. Compressive ratcheting strains existed in the axial direction at the extra-

dos (0°). However, the hoop direction at the intrados (180°) exhibited the largest ratcheting strain of 2.3%, while the largest ratcheting hoop strain range of about 2.2% occurred at the 90° location. This means that the fatigue-ratcheting induced crack most probably occurred at the 90° location because the cyclic strain range primarily dominated the fatigue mechanism. The hoopwise ratcheting primarily happened at the intrados and extrados locations. The basic ratcheting behavior predicted in this study agreed, in general, with that found in the limited physical tests in the literature. This parametric study, however, predicted more detailed ratcheting behavior with completed ratcheting strain values of interest for the practical input loads using the shell element model.

The analyses also predicted the largest ratcheted shear strains existing at the 90° location as shown in Fig. 9. The shear strains are important to examine the actual strain status of the elbow

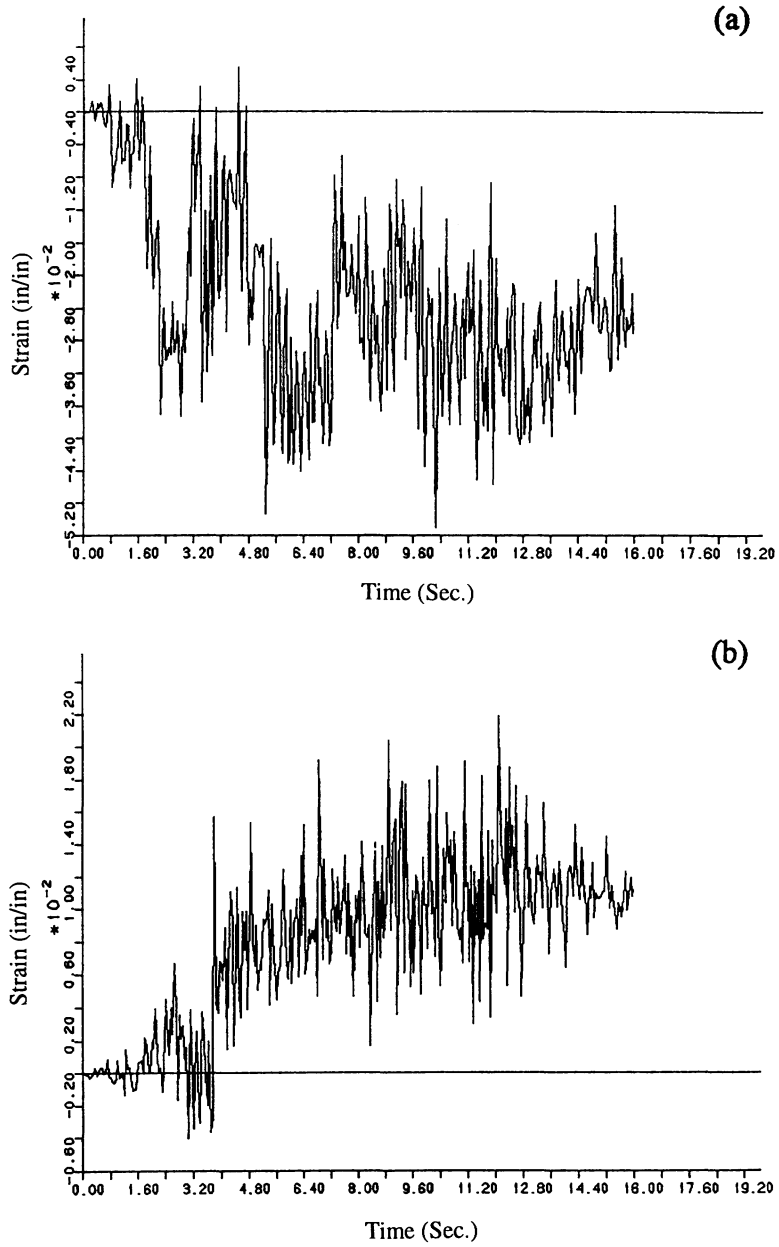

FIGURE 9 Shear strains at the (a) 90° and (b) 180° points on the cross section 45° away from the elbow end under actual cyclic loads.

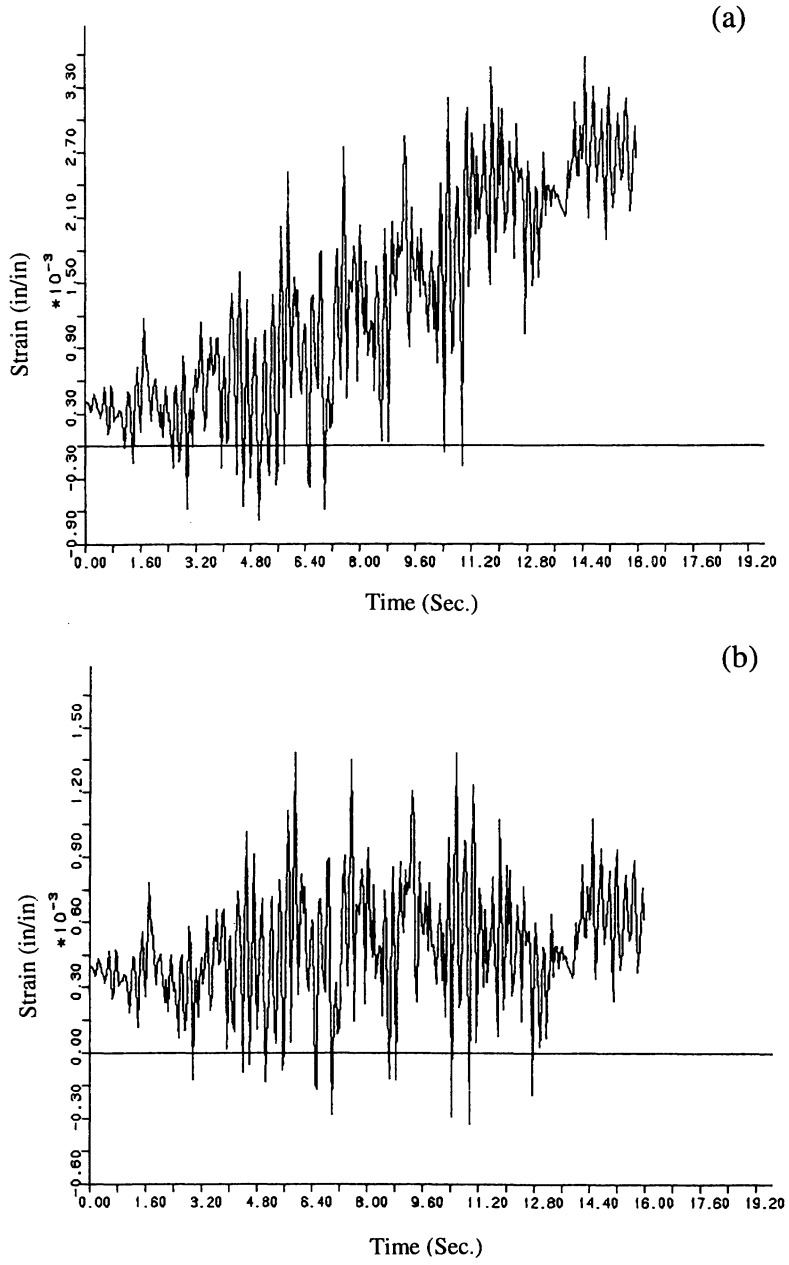

FIGURE 10 Cyclic loads scaled down (a) five and (b) 10 times, hoop strains at the 180° point on the cross section 45° away from the elbow end.

at that location, and may be induced by the unsymmetrical loads that often happen in practical piping and structural systems and cause unsymmetrical ovalizations in the elbows. This means that the potential fatigue induced crack at the 90° location may propagate in a direction between the axial and hoop directions rather than purely along the axial direction, as predicted by other researchers using a symmetrical elbow loaded by symmetrical pure bending. The actual crack propagation direction depends on load properties and structural dimensions.

For the case when the input cyclic displacement loads were scaled down five and 10 times and the internal pressure was equal to 1350 psi, the calculated hoop strains at the 0° and 180° points on the 45° symmetrical section (Fig. 5) are shown in Fig. 10. These results indicate that the ratcheting behavior exists only in the hoop direction at the intrados (180°) location for the case of

five times scaled down displacement loading. No ratcheting happens at other locations, primarily because the associated cyclic strains are less that the yield strain of 0.21% (corresponding to the yield stress of 60.1 ksi) for the SA-106B carbon steel at 200F.

For the case of 10 times scaled down displacement loading, the results, as expected to check the SOLVIA code, demonstrated that no ratcheting happened at all on the four typical points because the corresponding cyclic strains were less than the yield strain value. From the results mentioned above, a conclusion, as obtained by other researchers in the literature, was verified that the hoopwise ratcheting happens right after the nonzero mean cyclic strain values in the hoop direction exceed the yield strain. In this case the yield stress is equal to 0.21% for the SA-106B carbon steel at 200F.

When the cyclic displacement loads were scaled up two and three times (which is equivalent to scaling up the ground excitations to the same levels because the global random vibration analyses are linear and localized ratcheting, as observed in the physical tests, causes the larger deformation and load redistribution in some elbow areas and does not significantly affect the global stiffness of piping) and the pressure of 1350 psi remained unchanged, a compressive axial strain ratcheting existed only at the extrados location. The hoop strain ratcheting, in contrast to those with the actual cyclic loads, still happened at the intrados and extrados points but with larger values and higher accumulation rates. The hoop ratcheting strain was accumulated through the whole duration at the intrados point, and the maximum hoop ratcheting strain range was about 4.1 and 6% at the 90° point for these two loading cases. The largest ratcheted shear strain existed at the 90° location.

Figure 11 shows the calculated hoop strains at the typical location points (Fig. 5) when the displacement loads were scaled up four times and the internal pressure was equal to 1350 psi. The axial ratcheting was still compressive, occurring only at the extrados. The hoop ratcheting existed at the intrados and extrados points and "stopped" its accumulation when it exceeded about 4.4% as explained previously. The strain ratcheting stops probably due to using the prescribed displacement loading input plus the isotropic hardening rule. The plastic flow may stop when the peak displacements resulting in peak stresses are reached. This needs further investigation using force control and the kinematic hardening rule. However, the results predicted herein before the ratcheting stops are meaningful. The maximum hoop ratcheting range happens at the 90° points with a value of 8.0%. At the 90° point the largest shear strain exists as shown in Fig. 11.

Compared with the results in the pressure case of 1350 psi (Fig. 8), the strain results (as shown in Fig. 12 when the pressure is reduced to zero and increased to 7676 psi such that the pressure induced hoop stress is equal to one times the allowable design stress intensity value, S_h, for class 2 piping while the displacement loads remain unchanged) indicate that under the zero pressure loading case the axial and hoopwise strain ratcheting behavior still exists only at the extrados. At this point no significant magnitude changes in the axial ratcheting strain were found, while the hoopwise ratcheting strains were almost reduced two times. No hoopwise ratcheting existed for this case at the intrados. In contrast to the case of pressure equal to 1350 psi or the pressure hoop stress equal to $0.18S_h$ (as discussed previously and shown in Fig. 8), when the pressure was increased to 7676 psi, the hoopwise ratcheting strain ranges in this case were greatly reduced and more obvious ratcheting behavior appeared that was increased more than two times. The hoopwise ratcheting behavior occurred at all the four typical locations of 0°, 90°, 180°, and 270° with the largest ratcheting strains at the intrados. The ratcheting stops when the strains accumulate to about 5.8%, which is consistent with the experimental results obtained by General Electric (1990). The largest hoopwise ratcheting strain range of about 2.0% was found at the 90° point that was slightly smaller than that obtained when the pressure was equal to 1350 psi in Fig. 8. This means that the largest hoopwise ratcheting range value may not be affected by the changed value of internal pressure when the pressure hoop stress is above $0.18S_h$. The results obtained also show slight strain ratcheting in the axial direction.

The effects of yield stress were predicted as shown in Fig. 13, assuming it was equal to the nominal value of 35 ksi as specified by the ASME BPVC (1992) while the strain hardening modulus was kept the same as that accounted for in the previous loading cases. Under the same loads of the cyclic displacements and internal pressure as discussed previously and shown in Fig. 8, in contrast, Fig. 13 indicates that the lower the yield stress is, the higher the hoopwise ratcheted strain will be, and that the associated ratcheted strain

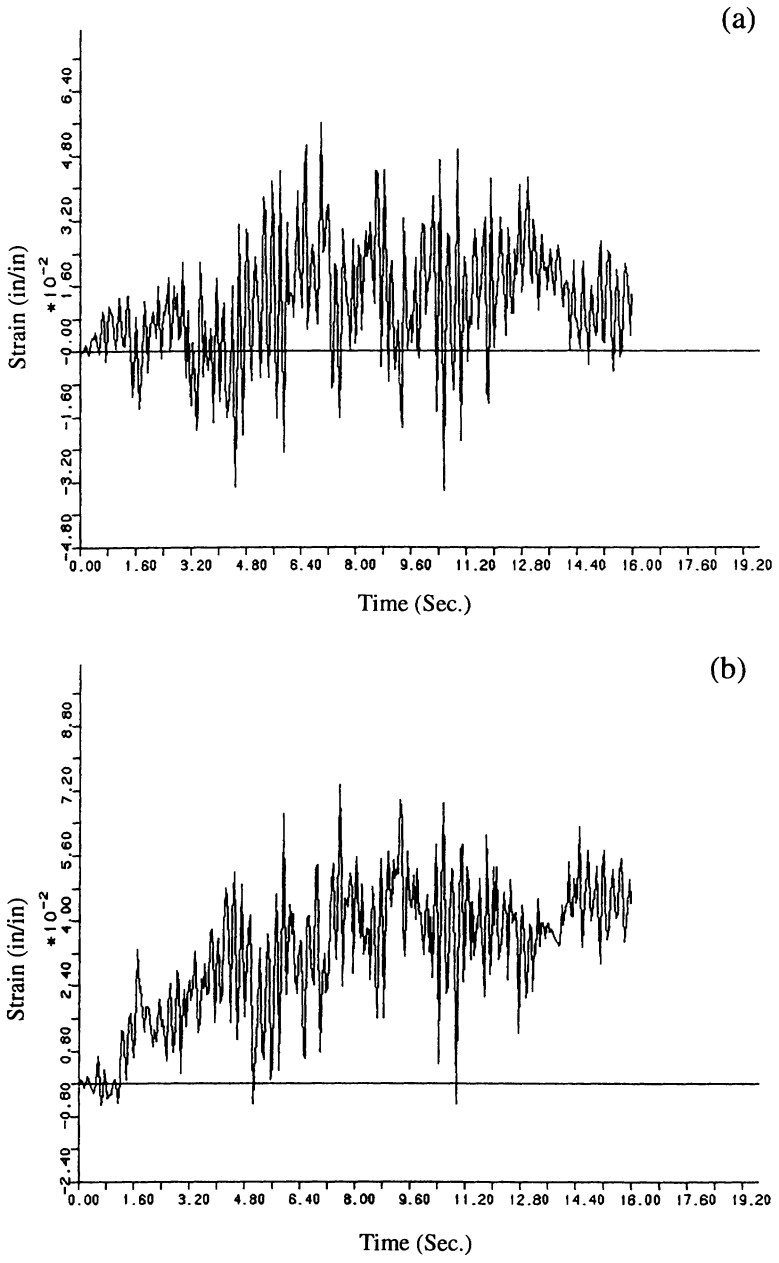

FIGURE 11 Hoop strain at the (a) 90° and (b) 180° points on the cross section 45° away from the elbow end when cyclic loads are scaled up four times.

time series under the two yield stress cases have similar shapes. This means that the ratcheting behavior of a strain time series shape may be determined primarily by the strain hardening, and that under the same load level the amplitude of the ratcheted strain may be dominated by the magnitude of the yield stress. In this reduced yield stress case the maximum hoop strain accumulation stops when the strain value exceeds about 3.4% at the intrados point. The largest hoop strain range of about 1.8% happens at the 90° point. Comparing the results before the yield stress was reduced, it was found that when the yield stress was reduced, the maximum hoop strain was increased while the maximum hoop strain range was decreased.

Figure 13 also shows the calculated hoop strain, assuming the regular tangent modulus of the bilinear ductile steel of 3.2×10^6 psi as shown in Fig. 4 is reduced two times to 1.6×10^6 psi to

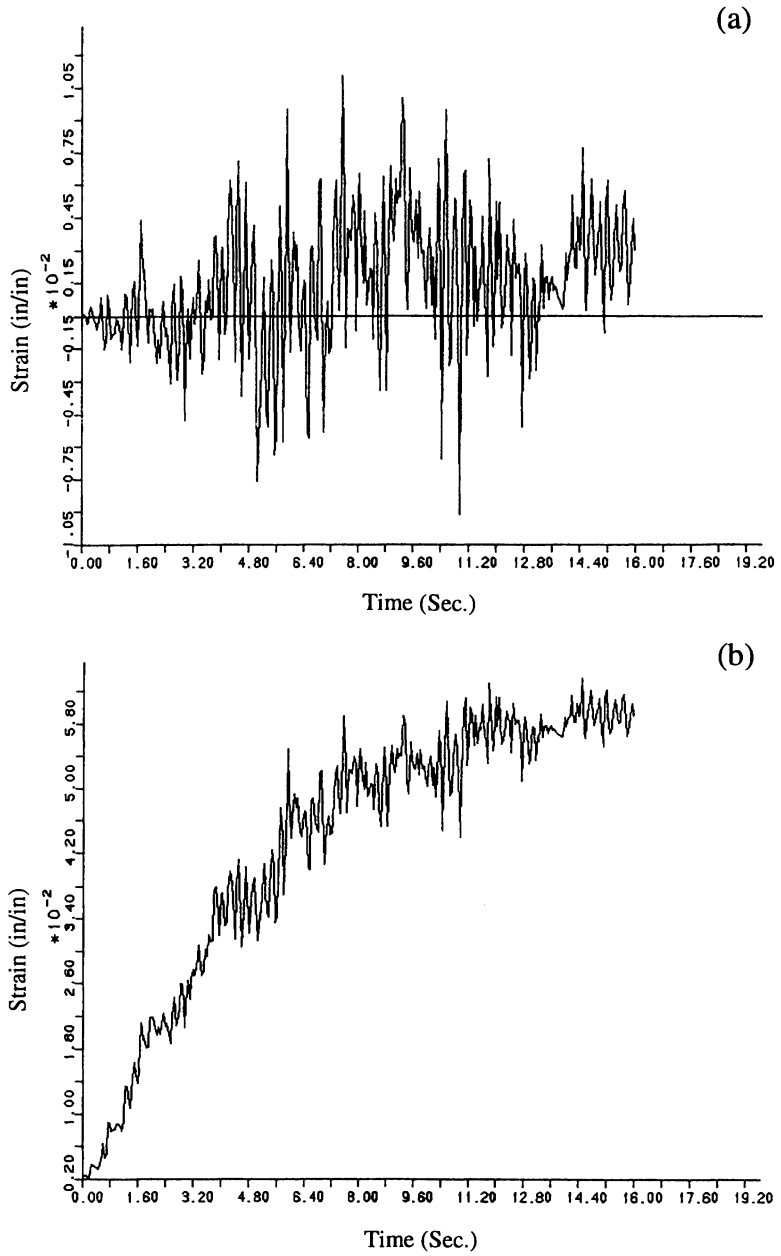

FIGURE 12 Pressure hoop stress equals (a) 0 and (b) $1.0S_h$ hoop strains at the 180° point on the cross section 45° away from the elbow end.

investigate the effects of material strain hardening to ratcheting. Comparing the axial and hoop strains obtained in this case with those when the tangent modulus is equal to 3.2×10^6 psi, it was found that:

1. the basic ratcheting behavior was similar between these two cases;
2. the largest hoop ratcheting strain of 2.2% at 7.2 s in this case versus 2.3% at 7.5 s in the regular case happened at the intrados (180°) separately, and the maximum hoop strains at the other three points also occurred earlier when the tangent modulus was equal to 1.6×10^6 psi than at 3.2×10^6 psi;
3. the 90° point exhibited the largest hoop strain range of 1.5% in this case versus 2.2% in the regular case; and
4. when loading beyond yield, the change in the tangent modulus caused load redistribu-

tions that increased or decreased the maximum axial or hoop strains at different points, and the strain hardening property of the elbow material controlled the plasticity flow in the elbow areas.

In reduced material strain hardening, the results obtained also showed the shear strains at the 90° and 180° points separately, which demonstrated that the largest shear strain was also at the 90° point as found when the tangent modulus was not reduced. The comparison of these two cases of material strain hardening indicated that the shear strain directions were reversed at the two points when the tangent modulus was reduced two times. This might have been caused by torsional effects due to the load redistributions in the elbow areas.

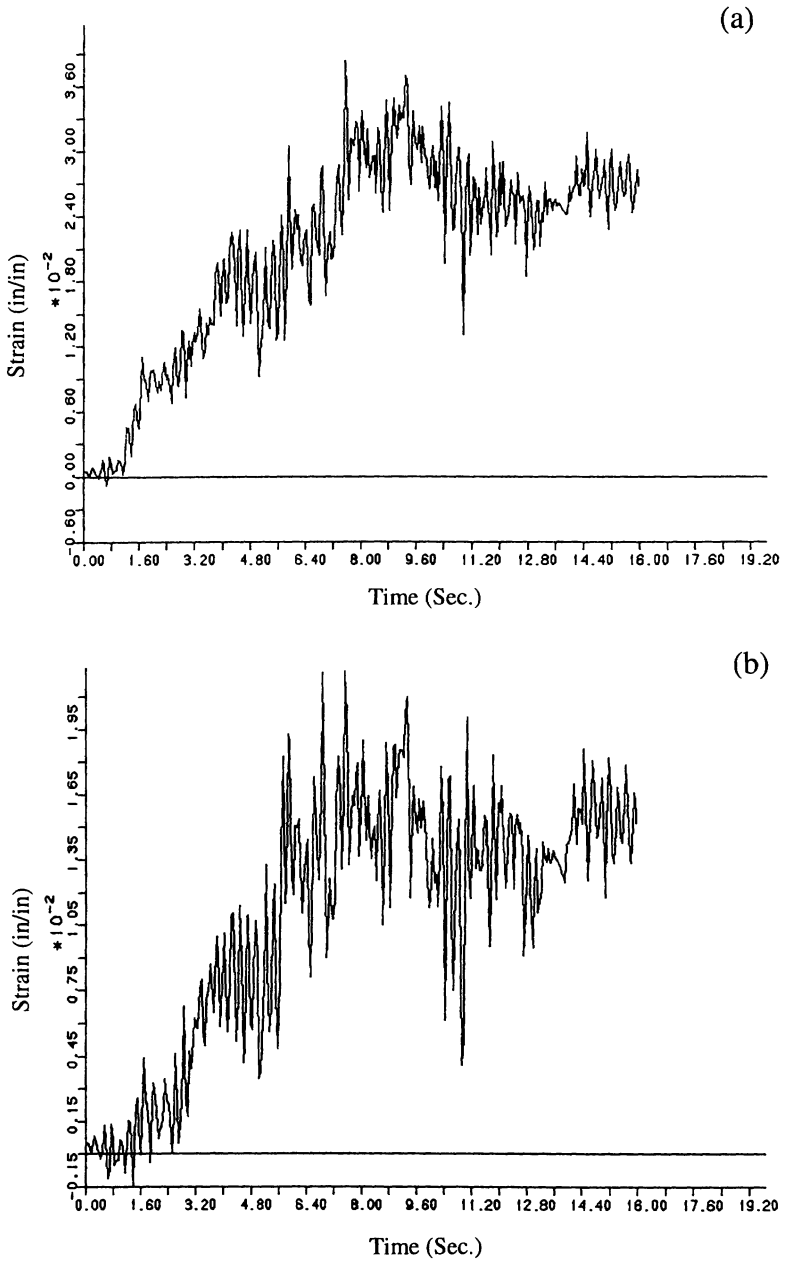

FIGURE 13 Hoop strains at the 180° point on the cross section 45° away from the elbow end (a) when yield stress equals 35 ksi and (b) when tangent modulus is reduced two times.

CONCLUSIONS

Parametric nonlinear finite element analyses were performed of large strain ratcheting in cyclic plasticity of a pressurized carbon steel pipe elbow loaded by a prescribed multiaxial stochastic displacement response time series. The basic ratcheting behavior predicted in this study agreed, in general, with that found in the limited physical tests in the literature. This parametric study, however, predicted more detailed ratcheting behavior with completed ratcheting strain values of interest for the practical input loads using the shell element model.

Some observations through this study are that:

1. In general, strain ratcheting (as reported in the literature) occurs when nonzero mean cyclic stress exceeds the yield stress of the ductile material in both the axial and hoop directions of the elbow.
2. The largest ratcheting strain occurs in the hoop direction at the intrados (180°) on the symmetrical cross section of the elbow. The maximum hoopwise ratcheting strain range occurs at the 90° location where potential ratcheting fatigue induced cracks may appear and propagate in a direction between the axial and hoop directions rather than purely in the axial direction. The significant shear ratcheting strain is caused by unsymmetrical loadings and structures.
3. Ratcheting rate significantly increases at lower load levels and slowly increases with an increment of load level.
4. The hoopwise ratcheting stops at strains of about 4.4 and 5.8%, respectively, when the pressure induced hoop stress is equal to 0.18 and 1.0 times the allowable design stress intensity value for ASME class 2 piping. This may be due to the combination of the prescribed displacement input and isotropic hardening rule. Whether ratcheting stops under some conditions could be verified using prescribed force input plus the more rational kinematic hardening rule. This is future work.
5. The curve shape of the ratcheting strain may be governed by material strain hardening, while the magnitude of the ratcheted strain may be dominated by material yield stress. The smaller the yield stress is, the lower the ratcheting strain value will be. The softer the material strain hardening or the smaller the tangent modulus is, the faster the ratcheting strain happens and the smaller the maximum hoop ratcheting strain range will be. The reduction of material strain hardening or tangent modulus causes significant load redistributions in the elbow areas when loading beyond yield.
6. The results obtained in this study may provide valuable insights of seismic safety margin issues of nuclear piping and can be used for a further evaluation of the ongoing ASME B&PV Section III Code changes (General Electric, 1990; Slagis, 1993; Zhao, 1993; Barnes et al., 1994).

The authors wish to thank Dr. Dario A. Gasparini for his valued comments, Mr. Paul R. Wilson for his assistance in performing the finite element analyses, and Ms. Jinping Zhao for her assistance in preparation of the manuscript. The major financial support from Electric Power Research Institute (EPRI) Grant RP2967-04 and partial financial support from S&A for this research project are gratefully acknowledged.

REFERENCES

American Society of Mechanical Engineers (ASME), 1992, *Boiler & Pressure Vessel Code (B&PVC)*, ASME, New York, Section III.

Azzam, T. J., and Scavuzzo, R. J., 1991, "Analysis of Ratcheting in Pressurized Pipe Elbows," *ASME PVP*, Vol. 220, pp. 107–116.

Azzam, T. J., 1992, "Ratcheting in Cyclically Loaded Pressurized Elbows," PhD Thesis, University of Akron, Akron, OH.

Barnes, R. W., Tagart, S. W., Branch, E. B., and Landars, D. F., 1994, "Proposed Revision to Section III Seismic Piping Rules," *ASME PVP*, Vol. 275-1, pp. 67–71.

Beaney, E. M., 1991, "Failure of Elbows under Seismic Loading," Report TD/SID/REP/0134, Berkeley Nuclear Laboratories, UK.

Boussaa, D., Van, K. D., Labbe, P., and Tang, H. T., 1993a, "Elastic-Plastic Bending of Pressurized Elbows," *ASME PVP*, Vol. 264, pp. 35–44.

Boussaa, D., Van, K. D., Labbe, P., and Tang, H. T., 1993b, "Fatigue-Ratcheting Analysis of Pressurized Elbows," *ASME PVP*. Vol. 266, pp. 13–21.

Box, G. E. P., and Jenkins, G.M., 1976, *Time Series Analysis: Forecasting and Control, rev. ed.*, Holden-Day, Oakland, CA.

Garud, Y. S., 1993, "Analysis and Prediction of Fatigue-Ratcheting: Comparison with Tests and Code Rules," *ASME PVP*, Vol. 266, pp. 23–32.

General Electric, 1990, "Piping and Fitting Dynamic Reliability Program," Preliminary Report under Electric Power Research Institute (EPRI) Contract RP-1543-15, Palo Alto, CA.

Jaquay, K. R., and Tang, H. T., 1991, "Post-Test Predictions of High Level Vibration Tests of Nuclear Piping," *Structural Mechanics in Reactor Technology (SMiRT) 11 Transactions,* Vol. K.

Kot, C. A., 1990, "SHAM: High-Level Seismic Tests of Piping at the HDR," *Nuclear Engineering and Design,* Vol. 118, pp. 305–318.

Kussmaul, K., 1987, "Investigation of the Plastic Behavior of Pipe Bends," *ASME PVP,* Vol. 127, pp. 55–61.

Park, Y. J., 1991, "The High Level Vibration Test Program," US Nuclear Regulatory Commission NUREG/CR-5585, Washington, DC.

Rockwell International, 1990, "A Simplified Inelastic Seismic Analysis Method for Piping Systems," *Electric Power Research Institute EPRI NP-6809,* Palo Alto, CA.

Scavuzzo, R. J., 1993, "Seismic Plastic Behavior of Piping," in Au-Yang, M. K., *Technology for the '90s, A Decade of Progress,* The ASME Pressure Vessels and Piping Division, New York, pp. 1093–1104.

Severud, L. K., 1988, "High Level Seismic Response and Failure Prediction Methods for Piping," *US Nuclear Regulatory Commission NUREG/CR-5023,* Washington, DC.

Shiao, C. Y., 1986, "Synthesis and Analysis of Random Process," *PhD Thesis,* Case Western Reserve University, Cleveland, OH.

Slagis, G. C., 1993, "Seismic Design of Nuclear Piping—Past, Present, and Future," in Au-Yang, M.K., *Technology for the '90s, A Decade of Progress,* The ASME Pressure Vessels and Piping Division, New York, pp. 983–1010.

SOLVIA Engineering AB, 1990, *User Manual of SOLVIA-90, Revision 90.2,* Ostra Ringvagen 4, S-722 14 Vateras, Sweden.

Tagart, S. W., and Ranganath, S., 1992, "Proposed Dynamic Stress Criteria for Piping," *ASME PVP,* Vol. 237-1, pp. 133–137.

Zhao, Y., 1993, "Random Vibration for Seismic Analysis of Multiply Supported Nuclear Piping," PhD Thesis, Case Western Reserve University, Cleveland, OH.